Electrosynthesis of ReS₄. XAS Analysis of ReS₂, Re₂S₇, and ReS₄

Daniel E. Schwarz,[†] Anatoly I. Frenkel,[*,‡] Ralph G. Nuzzo,[*,†]
Thomas B. Rauchfuss,[*,†] and Appathurai Vairavamurthy[§]

*Department of Chemistry and the Frederick Seitz Materials Research Laboratory,
University of Illinois at Urbana-Champaign, Urbana, Illinois 61801, Department of Physics,
Yeshiva University, 245 Lexington Avenue, New York, New York 10016, and Department of
Energy Sciences and Technology, Brookhaven National Laboratory, Upton, New York 11973*

Solutions of ReS_4^- undergo electro-oxidation at 0.5 V vs Ag|AgCl to give black, amorphous ReS_4 via a process that can be reversed at -0.9 V. The oxidative polymerization can also be effected chemically using either I_2 or ferrocenium as oxidants. X-ray absorption spectroscopy (XAS) suggests that the phases Re_2S_7 and ReS_4 are closely related structurally. The XAS data were calibrated with studies on $[ReS_4]^-$ and crystalline ReS_2. For both ReS_4 and Re_2S_7 XAS data show the presence of both S^{2-} and S_2^{2-}, with S^{2-} being less abundant than S_2^{2-}. The presence of terminal sulfides ($r_{Re=S} \sim 2.14$ Å) was ruled out by the EXAFS analysis. Variable temperature EXAFS studies showed that ReS_4 and Re_2S_7 convert to ReS_2 as anticipated from the results of TGA experiments. These considerations, when taken together with literature precedents, led to the reformulation of Re_2S_7 as $Re^V(S)_{1.5}(S_2)_1$, and correspondingly ReS_4 is formulated as $Re^V(S)_1(S_2)_{1.5}$. These two materials are proposed to be members of a continuum of $Re(S)_{1.5-1}(S_2)_{1-1.5}$ structures that differ in terms of their S_2^{2-}/S^{2-} ratio. Chain structures accommodate these considerations and are consistent with a largely reversible electrochemistry that regenerates ReS_4^-.

Introduction

Transition metal sulfides (TMS) are immensely useful materials. The preponderate motivation for their study is associated with the utility of MoS_2 and related materials as catalysts for the hydrodesulfurization (HDS) of petroleum.[1,2] TMS have also been exploited as candidates for secondary cathodes in batteries, technology that was commercialized in the case of the Li−TiS₂ battery.[3] Beyond these practical considerations, the binary sulfides have attracted considerable interest for their novel electronic properties, e.g., charge density waves, quantum size effects, and superconductivity.[4] A recent theory on the origin of life invokes a key role played by Fe−S and Fe−Ni−S species.[5,6] Driven by the intense interest in TMS, new binary phases continue to be discovered and new synthetic techniques introduced.[7−11] In the preceding 20 years, several new TMS materials have been described, including TaS₃,[12] Ta₃S₂,[13] $MoS_{4.7}$,[14] $MoS_{5.6}$,[15] and nanotubes of MS_2 (M = Ti, Mo, W).[10,16,17]

TMS can be classified according to their degree of sulfur−sulfur bonding. "Sulfur-rich" phases feature S−S bonding, usually in the form of persulfido units (S_2^{2-}), the most famous example being FeS_2. Some species, illustrated by TaS₃, have both per- and monosulfido units. A second broad class of TMS includes materials with isolated sulfide (S^{2-}) centers, e.g., MoS_2 and FeS. Metal-rich phases such as Ta₃S₂ exhibit extensive metal−metal bonding.[13] Phases with low sulfur−metal ratios are generally more thermally stable than the sulfur-rich phases; thus, they are more amenable to high temperature recrystallization techniques. The sulfur-rich phases, on the other hand, are often thermally labile with respect to the loss of sulfur, e.g., MoS_3 and Re_2S_7. Because such species are not readily crystallized, they are often characterized by X-ray absorption spectroscopy (XAS), specifically extended X-ray absorption

* Corresponding author.
† University of Illinois at Urbana-Champaign.
‡ Yeshiva University.
§ Brookhaven National Laboratory.
(1) Pecoraro, T. A.; Chianelli, R. R. *J. Catal.* **1981**, *67*, 430−445.
(2) Harris, S.; Chianelli, R. R. *J. Catal.* **1986**, *98*, 17−31.
(3) Benco, L.; Barras, J.-L.; Atanasov, M.; Daul, C.; Deiss, E. *J. Solid State Chem.* **1999**, *145*, 503−510.
(4) Jin, S.; Zhou, R.; Scheuer, E. M.; Adamchuk, J.; Rayburn, L. L.; DiSalvo, F. J. *Inorg. Chem.* **2001**, *40*, 2666−2674.
(5) Huber, C.; Wächtershäuser, G. *Science* **1997**, *276*, 245−247.
(6) Huber, C.; Wächtershäuser, G. *Science* **1998**, *281*, 670−672.
(7) Gillan, E. G.; Kaner, R. B. *Chem. Mater.* **1996**, *8*, 333−343.
(8) Ramli, E.; Rauchfuss, T. B.; Stern, C. L. *J. Am. Chem. Soc.* **1990**, *112*, 4044−4045.
(9) Dusastre, V.; Omar, B.; Parkin, I. P.; Shaw, G. A. *J. Chem. Soc., Dalton Trans.* **1997**, *19*, 3505−3508.
(10) Tenne, R. *Prog. Inorg. Chem.* **2001**, *50*, 269−315.

(11) Axtell, I., E.; Liao, J.-H.; Kanatzidis, M. G. *Inorg. Chem.* **1998**, *37*, 5583−5587.
(12) Meerschaut, A.; Guemas, L.; Rouxel, J. *J. Solid State Chem.* **1981**, *36*, 118−123.
(13) Kim, S. J.; Nanjundaswamy, K. S.; Hughbanks, T. *Inorg. Chem.* **1991**, *30*, 159−164.
(14) Hibble, S. J.; Rice, D. A.; Pickup, D. M.; Beer, M. P. *Inorg. Chem.* **1995**, *34*, 5109−5113.
(15) Afanasiev, P.; Bezverkhy, I. *Chem. Mater.* **2002**, *14*, 2826−2830.
(16) Feldman, Y.; Wasserman, E.; Srolovitz, D. J.; Tenne, R. *Science* **1995**, *267*, 222−225.
(17) Mastai, Y.; Homyonfer, M.; Gedanken, A.; Hodes, G. *Adv. Mater.* **1999**, *11*, 1010−1013.
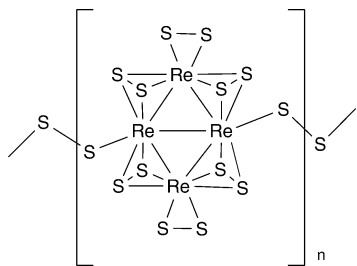
Figure 1. Structure proposed for Re_2S_7 from initial EXAFS analyses.[26,27]

fine structure (EXAFS) and X-ray absorption near-edge structure (XANES).

The sulfides of Re[18] have attracted recent attention because Re–S compositions are particularly active HDS and hydrogenation catalysts.[19,20] Single crystal X-ray diffraction has shown that ReS_2 adopts a $CdCl_2$ structure distorted by a Re–Re bonding network.[21,22] Interestingly, ReS_2 obeys the 18e rule, when one includes the contributions of the localized Re–Re bonding. Beyond ReS_2, the only other generally accepted sulfide of rhenium is Re_2S_7, which has been used for the hydrogenation of difficult substrates that poison Pt metal catalysts, e.g., NO and SO_2.[23] A mineral identified as ReS_x ($2 < x < 3$) has been reported but not characterized crystallographically.[24]

Dirhenium heptasulfide forms upon the acidification of solutions of the perthiorhenate ion ReS_4^- as well as by treatment of Re_2O_7 with H_2S.[25] Hibble et al. have examined Re_2S_7 by Re- and S-XANES and EXAFS.[26,27] These workers suggest that Re_2S_7 consists of persulfido ligands exclusively, i.e., $Re_4(S_2)_7$ (Figure 1). Patterns in the structural chemistry of metal sulfides suggest that this structural proposal would be highly unusual. For example, the oxidation state of $Re^{3.5+}$ is lower than even ReS_2. A reinvestigation of this material is reported herein.

The present project began with a study of the redox properties of ReS_4^-, whose metallo-organic chemistry we have recently described.[28-31] Schäfer et al. showed that ReS_4^- undergoes sequential reductions at -1.58 and -2.46 V vs $Fc|Fc^+$,[32] and Ciurli et al. reported these

values as -1.12 and -1.99 V vs SCE.[33] The oxidation of ReS_4^- has not been previously explored, although we show here that it provides access to a novel sulfur-rich material.

Experimental Section

Materials and Methods. Elemental analyses and thermogravimetric analysis (TGA) were conducted at the School of Chemical Sciences Microanalysis Laboratory. TGA measurements were performed on a Perkin-Elmer TGA7 and were conducted under an atmosphere of nitrogen or helium. Scanning electron microscopy (SEM) and X-ray energy dispersive spectroscopy (XEDS) were performed on a Zeiss DSM 960 at the Frederick Seitz Material Research Laboratory. Et_4NReS_4 was prepared following our recent modification of a method described by Exxon.[34] ReS_2 was purchased from Cerac and was examined by powder X-ray diffraction and inductively coupled plasma (ICP) elemental analysis. Anal. Calcd for ReS_2 (found): Re, 74.38 (75.37); S, 25.62 (25.65). The manufacturer provided corroborating powder X-ray diffraction and elemental analysis data. Re_2S_7 was purchased from Aldrich; powder X-ray diffraction analysis showed that this material was indeed amorphous. Anal. Calcd for Re_2S_7 (Found): Re, 62.39 (62.01); S, 37.61 (35.40).

Chemical Synthesis of ReS_4 by I_2 Oxidation. A solution of 0.531 g (1.19 mmol) of Et_4NReS_4 in 30 mL of MeCN was added dropwise to a solution of 0.093 g (0.733 mmol) of I_2 in 30 mL of MeCN. A black precipitate formed immediately. The solid was collected by filtration and washed with MeCN and Et_2O and dried in vacuo. Yield: 0.22 g (60%). Anal. Calcd (Found) for ReS_4: C, 0 (5.25); H, 0 (0.88); N, 0 (1.07); Re, 55.39 (50.48). Attempts to remove the CHN impurities involved grinding the material in a N_2 box followed by a Soxhlet extraction in MeCN for 12 h which provided a material with a lower CHN content. Anal. Calcd (Found) for ReS_4: C, 0 (4.91); H, 0 (0.80); N, 0 (0.59); Re, 59.21 (54.40).

Chemical Synthesis of ReS_4 by Fc^+ Oxidation. A solution of 0.505 g (1.13 mmol) of Et_4NReS_4 in 30 mL of MeCN was slowly added over 5 min to a solution 0.30 g (0.91 mmol) of $(Cp_2Fe)[PF_6]$ in 30 mL of MeCN. The resulting black precipitate was collected by filtration and washed with MeCN and Et_2O and dried in vacuo. Yield: 0.20 g (59%). Anal. Calcd (found) for ReS_4: C, 0 (3.75), H, 0 (0.37), N, 0 (0.38), Re, 55.39 (55.14). Attempts to remove the CHN impurities involved grinding the material in a N_2 box followed by Soxhlet extraction with MeCN for 12 h, which provided a material with a lower CHN content. Anal. Calcd (Found) for ReS_4: C, 0 (3.06); H, 0 (0.36); N, 0 (0.0); Re, 59.21 (55.24).

Electrochemical Synthesis of ReS_4. The cyclic voltammetry experiments were performed with a Bioanalytical System BAS-CV 50W electrochemical analyzer in an N_2-purged 10 mL single compartment glass cell. The working electrode was either glassy carbon or Pt foil. The reference electrode was a Ag|AgCl, KCl (satd) electrode, and the counter electrode was Pt wire.

In one experiment, a stirred 4 mM solution of Et_4NReS_4 in 8 mL of MeCN (0.1 M Bu_4NPF_6) was maintained at 0.6 V vs Ag|AgCl for 2 min. After this time, a black coating had accumulated on the Pt electrode. The reversibility of the electrodeposition was demonstrated by removing the coated electrode and rinsing it in air with MeCN, inserting the electrode into a fresh MeCN solution (0.1 M Bu_4NPF_6), and applying a potential of -900 mV which resulted in the black layer dissolving over 30 s and providing a faint purple solution. The presence of ReS_4^- in solution was confirmed by UV–vis spectroscopy ($\lambda_{max} = 508$ nm).

Bulk electrochemical synthesis was performed in a 100 mL cell with a piece of 2 cm² Pt foil as the working electrode. The

(18) Saito, T. *J. Chem. Soc., Dalton Trans.* **1999**, 97−105.

(19) Stiefel, E. I. *ACS Symp. Ser.* **1996**, *653*, 2−38.

(20) Topsøe, H.; Clausen, B. S.; Massoth, F. E. *Hydrotreating Catalysis, Science and Technology*; Springer-Verlag: Berlin, 1996.

(21) Kelty, S. P.; Ruppert, A. F.; Chianelli, R. R.; Ren, J.; Whangbo, M. H. *J. Am. Chem. Soc.* **1994**, *116*, 7857−7863.

(22) Murray, H. H.; Kelty, S. P.; Chianelli, R. R.; Day, C. S. *Inorg. Chem.* **1994**, *33*, 4418−4420.

(23) Slaugh, L. H. *Inorg. Chem.* **1964**, *3*, 920−921.

(24) Korzhinsky, M. A.; Tkaschenko, S. I.; Schmulovich, K. I.; Taran, Y. A.; Steinberg, G. S. *Nature* **1994**, *369*, 51−52.

(25) Briscoe, H. V. A.; Robinson, P. L.; Stoddart, E. M. *J. Chem. Soc.* **1931**, 1439−1443.

(26) Hibble, S. J.; Walton, R. I.; Feaviour, M. R.; Smith, A. D. *J. Chem. Soc., Dalton Trans.* **1999**, 2877−2883.

(27) Hibble, S. J.; Walton, R. I. *J. Chem. Soc., Chem. Commun.* **1996**, 2135−2136.

(28) Goodman, J. T.; Inomata, S.; Rauchfuss, T. B. *J. Am. Chem. Soc.* **1996**, *118*, 11674−11675.

(29) Goodman, J. T.; Rauchfuss, T. B. *Angew. Chem., Int. Ed. Engl.* **1997**, *36*, 2083−2085.

(30) Goodman, J. T.; Rauchfuss, T. B. *Inorg. Chem.* **1998**, *37*, 5040−5041.

(31) Goodman, J. T.; Rauchfuss, T. B. *J. Am. Chem. Soc.* **1999**, *121*, 5017−5022.

(32) Schäfer, R.; Kaim, W.; Moscherosch, M.; Krejcik, M. *J. Chem. Soc., Chem. Commun.* **1992**, 834−835.

(33) Ciurli, S.; Carney, M. J.; Holm, R. H.; Papaefthymiou, G. C. *Inorg. Chem.* **1989**, *28*, 2696−2698.

(34) Goodman, J. T.; Rauchfuss, T. B. *Inorg. Synth.* **2002**, *33*, 107−110.

saturated solution of Et_4NReS_4 in MeCN (0.1 M Bu_4NPF_6) was held at 0.6 V vs Ag|AgCl for 100 s. The electrode was then removed and washed with MeCN and dried in air. The black material was removed from the electrode with a razor blade and thoroughly dried in vacuo overnight. Analysis by XEDS confirmed the Re/S ratio of 1:4. Found (Theory): Re, 59.51 (59.21); S, 40.49 (40.79). XEDS over several parts of the sample confirmed its uniformity. IR analysis in the 4000−700 cm⁻¹ range showed no prominent absorptions.

Samples for XAS. Samples for XAS analysis were ground in a N_2 atmosphere and passed through a 200 mesh sieve. The powder was then mixed thoroughly with an equal weight of carbon black. About 25 mg of the mixture was pressed into a rectangular wafer using a hydraulic press. The wafers were approximately 0.5 mm thick, thereby satisfying the condition that $\Delta\mu x \leq 1$, where x is the effective sample thickness and $\Delta\mu$ is the jump in absorption coefficient at the Re L_{III} absorption edge (10 534 eV). The samples were then mounted on the vertical stage in a custom-built variable temperature cell,[35,36] which is suited for simultaneous in situ X-ray fluorescence and transmission measurements. The in-situ cell was purged with helium for >1 h prior to heating the samples. Elevated temperature measurements were conducted under a flowing helium atmosphere. The temperature was monitored with a chromel/alumel thermocouple (Omega) attached directly to the sample mounting stage. The sample was allowed to equilibrate for a minimum of 1 h at each temperature prior to data collection. Acetonitrile solutions of Et_4NReS_4 were studied only at room temperature and under argon in a custom-designed liquid sample cell with an exposed solution volume of 0.25 mL (dimensions 25 × 5 × 2 mm³).

XAS Measurements. The EXAFS measurements were obtained at the beamline X16C of the National Synchrotron Light Source (Brookhaven National Laboratory, Upton, NY). The X16C beamline uses a sagittally focusing double-crystal monochromator with Si(111) crystals which focus 3.5 mrad of light into a 0.3 × 0.5 mm² beam spot at the sample. The intensity of the focused beam (I_0) was measured with a 15 cm long ion chamber filled with a 10:1 mixture of He/Ar. X-ray absorption data from the sample were measured primarily in transmission mode by scanning from 200 eV below to 1000 eV above the Re L_{III} edge. A 30 cm long Ar-filled ion chamber placed after the sample, collinear with the beam, was used to measure the transmission beam intensity, I_t. The Et_4NReS_4 solution X-ray absorption data was measured in both transmission and fluorescence modes. This was accomplished by turning the solution cell containing the sample to ~45° with respect to the beam direction and measuring the intensity of the transmitted (I_t) X-rays and the intensity of the X-ray fluorescence (I_f) from the sample. A 4 cm long, Ar-filled ion chamber (Lytle detector) placed at 90° with respect to the beam direction was used to measure I_f. A standard, thin Re metal foil was used to calibrate the beam energy during each Re L_{III}-edge XAS scan for all samples. The calibration measurement was made with the reference ion chamber (I_r) placed downstream of I_t. The measurements of the absorption coefficient near the Re L_{III} edge in pure Re were taken simultaneously with the samples of interest by placing the Re metal standard between the ion chambers I_t and I_r, and measuring the absorption coefficient in I_r due to the metal standard. The characteristic features of the absorption coefficient in pure Re were later used to accurately calibrate (0.3 eV or better) the X-ray energy of each scan.

In situ temperature measurements were performed by heating the sample with a resistor heater while flowing He gas at 40 mL/min over the sample. The setup and experimental conditions, overall, were very similar to other in situ reaction measurements performed at this beamline during the recent years.[36−38]

EXAFS Data Analysis. Our analysis procedure was tested on ReS_2 and Et_4NReS_4; both of these compounds have been structurally characterized by single crystal X-ray diffraction (see Introduction) and thus are suitable reference compounds. The ion ReS_4^- is a molecular species and therefore quite different from ReS_4, which is expected to be a structurally complex extended solid. The structural model for ReS_2 was constructed using the coordinates from Murray et al.'s crystallographic study,[22] which contains two inequivalent Re sites in the unit cell, each octahedrally coordinated by sulfur atoms. The Re−S bond lengths in ReS_2 range from 2.31 to 2.50 Å, the average length being 2.40 Å. For each Re site, the six nearest Re−Re neighbors are divided into two groups with respect to their lengths, three in each group. These Re−Re lengths fall into two distinct ranges, one group of three Re−Re pairs (from 2.69 to 2.90 Å) is centered around 2.80 Å, and the second group of three Re−Re pairs (from 3.56 to 3.77 Å) is centered around 3.68 Å. This variety of bond lengths is a result of the sulfur being situated above or below three, two, one, or zero Re−Re bonds. For our fitting procedure, the Re−S interactions were modeled theoretically using FEFF6,[39] using calculations based on the atomic coordinates of the ReS_2 structure. A theoretical, 6-fold degenerate Re−S contribution to the first shell, with the bond length of 2.40 Å, was calculated and chosen to simulate the entire Re−S shell by varying the correction to the model bond length, the mean square bond lengths disorder (σ^2), and the coordination number of the pair. Similarly, two theoretical contributions were constructed with FEFF6 for two groups of Re−Re distances. To fit more Re−Re contributions to the EXAFS data, their bond lengths, disorder, and coordination numbers were varied in the fits as well. To analyze the data with FEFF theory, we used the UWXAFS[40] data analysis package (programs AUTOBK and FEFFIT) that utilizes the nonlinear least-squares fitting of EXAFS theory to the data and evaluates the uncertainties in the results.

Results

Electrochemistry of ReS₄. Using cyclic voltammetry, we confirmed the previously reported $ReS_4^{-/2-}$ couple at −1120 mV (vs SCE, Figure 2).[33] In the anodic scan direction, we observed a previously unreported oxidation wave at 0.5 V. This irreversible oxidation process is coupled to a (reductive) stripping peak at −0.9 V. The stripping peak was not observed unless the potential was first swept to ≥0.5 V. If, however, the oxidation of ReS_4^- was taken to very positive potentials, a large event is observed at 1.6 V, and the stripping peak at −0.9 V was no longer observed.

The electrodeposition proved to be reasonably reversible. In a typical reaction, the coated electrode could be removed from the electrolyte solution, rinsed with MeCN, and re-reduced at −900 mV in a fresh electrolyte solution to cleanly regenerate ReS_4^-, which was confirmed by optical measurements. In a coulommetry experiment, an 8 mM solution of Et_4NReS_4 in MeCN was first swept from −100 to 700 mV (25 mV·s⁻¹), and the second segment swept from 700 to −1500 mV. Under these conditions, −1.58 × 10⁻⁴ C and 9.92 × 10⁻⁵ C were transferred, respectively, for a stripping efficiency of 63%. The deviation from unity can be partially attributed to delamination of the deposited ReS_4 material from the electrode.

(35) Nashner, M. S.; Frenkel, A. I.; Adler, D. L.; Shapley, J. R.; Nuzzo, R. G. *J. Am. Chem. Soc.* **1997**, *119*, 7760−7771.

(36) Nashner, M. S.; Frenkel, A. I.; Somerville, D.; Hills, C. W.; Shapley, J. R.; Nuzzo, R. G. *J. Am. Chem. Soc.* **1998**, *120*, 8093−8101.

(37) Rodriguez, J. A.; Hanson, J. C.; Frenkel, A. I.; Kim, J. Y.; Perez, M. *J. Am. Chem. Soc.* **2002**, *124*, 346−354.
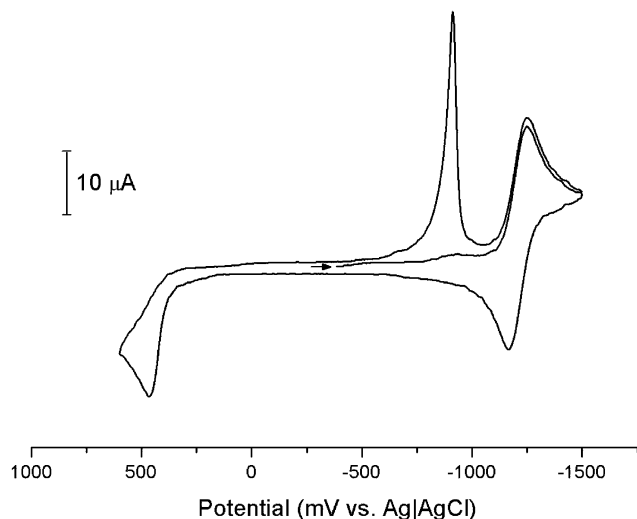
(38) Frenkel, A. I.; Hills, C. W.; Nuzzo, R. G. *J. Phys. Chem. B* **2001**, *105*, 12689−12703.

(39) Zabinsky, S. I.; Rehr, J. J.; Aukudinov, A.; Albers, R. C.; Eller, M. J. *Phys. Rev. B: Condens. Matter* **1995**, *52*, 2995−3009.

(40) Stern, E. A.; Newville, M.; Ravel, B.; Yacoby, Y.; Haskel, D. *Physica B (Amsterdam)* **1995**, *208−209*, 117−120.

Figure 2. Cyclic voltammogram of 0.6 mM solution of Et_4-$NReS_4$ in MeCN (0.1 M Bu_4NPF_6). The sweep rate was 100 mV/s.

Bulk Preparation of ReS_4. Prolonged oxidation of MeCN solutions of Et_4NReS_4 at 0.5 V in a stirred solution produced a thick black deposit on the working electrode (Pt foil). This solid, which was easily removed by scraping, proved to be amorphous on the basis of X-ray powder diffraction measurements. XEDS measurements showed that the solid retained its Re/S ratio of 1:4.

We also generated ReS_4 via chemical methods. Both I_2 and $[Cp_2Fe]PF_6$ effect the oxidation, consistent with their redox potentials of 0.75 and 0.5 V vs Ag|AgCl, respectively. We intentionally employed a deficiency of oxidants in order to minimize entrainment of impurities in the resulting solid; the electrochemically synthesized material was of higher purity. Elemental analysis indicated that the chemically produced material contained $10-15\%$ CHN, probably occluded Et_4NI or Cp_2-Fe. Soxhlet extraction of these solids with MeCN reduced the level of impurities to $3-5\%$.

Re L_{III}-Edge EXAFS. Given the amorphous nature of ReS_4, we turned to XAS measurements to obtain structural information on this material. ReS_2, Re_2S_7, and ReS_4 (synthesized by Fc^+ and electrochemical oxidation) were analyzed using nearly identical conditions. Data for Et_4NReS_4 were measured in an MeCN solution by both transmission and fluorescence modes.

Our EXAFS data for ReS_2 was satisfactorily fit using only three contributors (single scattering paths) to the EXAFS: six Re—S paths of half path lengths (the interatomic distances) of 2.40 Å, three Re—Re paths at 2.82 Å, and three Re—Re paths at 3.70 Å. Because the structure of ReS_2 is known, we did not vary coordination numbers in the fits. Our fits were good for EXAFS distances <3 Å, where two nearest neighboring shells contributed to the data (six Re—S pairs and the first group of three Re—Re pairs). The misfit in the higher r range is caused by our neglecting further neighbors, i.e., ones lying beyond the Re—Re shell. As a consequence, we do not analyze the data for contributors residing >3 Å in r-space. We do, however, include the second Re—Re group to fit ReS_2 data, in order to improve the quality of the fit in the low r region.

We have fixed the coordination numbers of Re—S and Re—Re contributions in the ReS_2 fits as 6 and 3,

Table 1. Comparison of Distances and Coordination Numbers (CN) for ReS_2 Deduced from Crystallographic,[22] EXAFS from Hibble et al.,[27] and the Present EXAFS Data

	Re—S [Å]	Re—Re [Å]	CN (Re—S)	CN (Re—Re)	σ^2 (Re—S) [Å²]	σ^2 (Re—Re) [Å²]
XRD	2.3976	2.803	6	3		
Hibble	2.362(2)	2.759(3)	6.0(2)	3.2(5)	0.0134(5)	0.015(1)
this work	2.389(7)	2.81(1)	6[a]	3[a]	0.0059(4)	0.007(1)

[a] CN values in EXAFS fits were fixed to be those from the XRD measurements.

Table 2. Comparison of EXAFS Data for Re_2S_7

	Re—S [Å]	Re—Re [Å]	CN (Re—S)	CN (Re—Re)	σ^2 (Re—S) [Å²]	σ^2 (Re—Re) [Å²]
Hibble[27]	2.325(2)	2.739(3)	5.0(2)	2.8(4)	0.0182(7)	0.0156(1)
this work	2.354(7)	2.76(1)	5.6(7)	1.7(5)	0.009(2)	0.006(3)

respectively, in agreement with the crystallography, in order to find the best fit value of the passive electron reduction factor ($S_0^2 = 0.80(4)$) that correlates with coordination numbers. S_0^2 was subsequently fixed equal to 0.80 for the rest of the EXAFS data fits where the coordination numbers were varied.

Our analyses, and that from Hibble et al.[27] for ReS_2, were based on previously published crystallographic coordinates.[22] The interatomic distances deduced in each of these studies are presented in Table 1; the results from this study are in slightly better agreement with the crystallographically determined distances than those reported by Hibble.

The ReS_2 data analysis was performed by using k^2-weighting to obtain both Re—S and Re—Re distances by simultaneously fitting FEFF theories of these pairs to the EXAFS data in r-space. This procedure was successful due to the relatively small number of fitting parameters. However, in the samples with unknown number of neighbors of each type, the difference in backscattering amplitudes $f(k)$ of Re—S and Re—Re photoelectron paths complicates the analysis. Namely, $f(k)$ for Re—S path contributes more strongly to the shorter k-range of the EXAFS data than that for Re—Re path, since Re is a stronger scatterer than S. We obtained better results by emphasizing the contribution of each bonding pair by using different k^n-weightings (k^2 or k^3) to fit Re—S and Re—Re contributions, respectively. We first used k^2-weighting to Fourier transform both EXAFS data and FEFF theory in order to refine the Re—S contribution to the data that affects the lower k-range stronger than Re—Re contribution. In this round of the analysis, we fit both theoretical contributions, Re—S and Re—Re, to the data simultaneously, using the r-range from 1.6 to 3.1 Å. Second, we subtracted theoretical Re—S contribution from the data and analyzed the resultant differential signal by fitting the Re—Re contribution in r-range from 2 to 3.2 Å using k^3-weighting for both the data and FEFF theory to further suppress any unsubtracted Re—S contributions and emphasize Re—Re contributions. The results are summarized in the Tables $1-5$. The EXAFS data and fits are displayed in Figures $3-5$. A similar analysis protocol has been used successfully to analyze separately the Nb—Nb and Nb—O contributions to the structure of $KNbO_3$, a material whose EXAFS data suffers from the same problem as described above.[41]

A sample of Et_4NReS_4 was measured as a MeCN solution by fluorescence EXAFS. These data were fit

Electrosynthesis of ReS₄

Chem. Mater., Vol. 16, No. 1, 2004 **155**

Table 3. Comparison of Bond Lengths (Å) and Coordination Numbers (CN) between ReS_2 and the Decomposition Products of Re_2S_7 and ReS_4 at 723 K

	Re−S [Å]	Re−Re [Å]	CN (Re−S)	CN (Re−Re)	σ^2 (Re−S) [Å²]	σ^2 (Re−Re) [Å²]
ReS_2	2.38(1)	2.80(3)	6	3	0.0076(7)	0.009(3)
Re_2S_7	2.379(7)	2.76(1)	6.3(5)	2.6(5)	0.009(1)	0.010(2)
ReS_4	2.379(7)	2.81(3)	5.7(3)	1.7(1.5)	0.0077(7)	0.010(4)

Table 4. EXAFS Data for Re_2S_7 and Its Decomposition Products at 300, 473, 598, and 723 K

	300 K	473 K	598 K	723 K
Re−S [Å]	2.354(7)	2.35(1)	2.34(1)	2.379(7)
Re−Re [Å]	2.76(1)	2.759(9)	2.75(1)	2.76(1)
CN (Re−S)	5.6(7)	5.2(5)	6.1(6)	6.3(5)
CN (Re−Re)	1.7(5)	1.4(2)	3.5(8)	2.6(5)
σ^2 (Re−S) [Å²]	0.009(2)	0.008(1)	0.009(1)	0.007(6)
σ^2 (Re−Re) [Å²]	0.006(3)	0.004(1)	0.008(2)	0.010(2)

using the Re−S path only. From the best fit, we determined the Re−S distance to be 2.13(1) Å and a Re−S coordination number of 3.5(7). The actual bond distance as determined by single crystal X-ray crystallography averages to 2.126(5) Å.[42] Note that the model correctly predicted the bond distance even though there are no Re=S bonds in ReS_2.

Our Re L_{III}-edge results on Re_2S_7 and ReS_4, together with data previously reported by Hibble et al. on Re_2S_7, are shown in Table 2. Regarding Re_2S_7, the Re−Re and Re−S bond distances determined by us are close to those previously reported. The occurrence of terminal Re=S bonds was ruled out. In particular, our model excludes such short Re−S bonds (ca. 2.15 Å[33]) because the resulting σ^2 would be quite large ($\sim$0.15 Å²). A unimodal distribution of Re−S bond lengths, as opposed to a bimodal one, is the only scenario consistent with experimental observations.
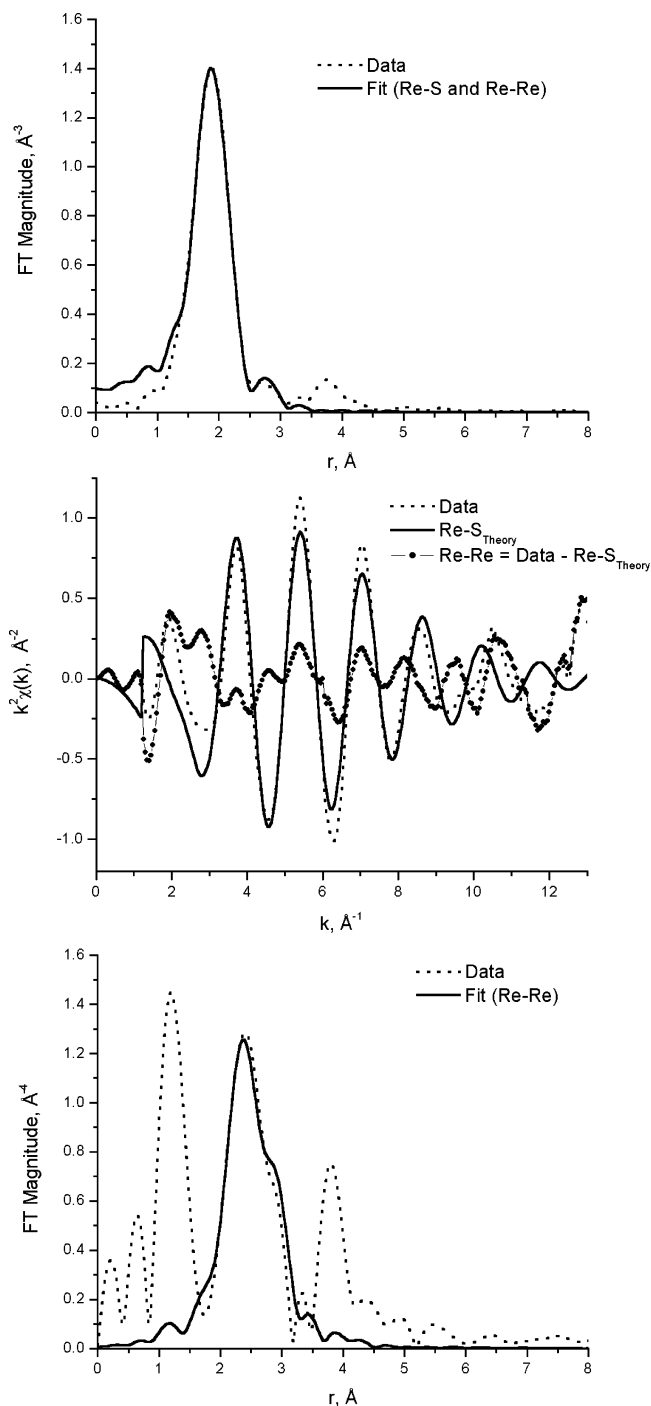
Our analysis suggested fewer Re−Re pairs (1.7(5) vs 2.8(4)) than previously reported. In this context it is important to note that in our work we were able to emphasize the contribution of Re−Re bonds to the total EXAFS spectrum by k^3-weighting procedure. This two-step fitting procedure leads to a more reliable set of coordination numbers and distances than the one-step fitting process adopted in the earlier work. The reliability of the analysis was indicated by the close similarity of the data obtained for pristine ReS_2 and a sample of the same derived by thermal decomposition of Re_2S_7 at 723 K (see below).

Sulfur K-Edge XANES Measurements. Sulfur K-edge XANES spectra provide characteristic "fingerprint" information on the redox state of the sulfur because of the sensitivity of XANES to the oxidation state of sulfur and its electronic environment.[43−45] The energy position of the main XANES peak, which represents a core-level s−p transition, shifts by about 1.25
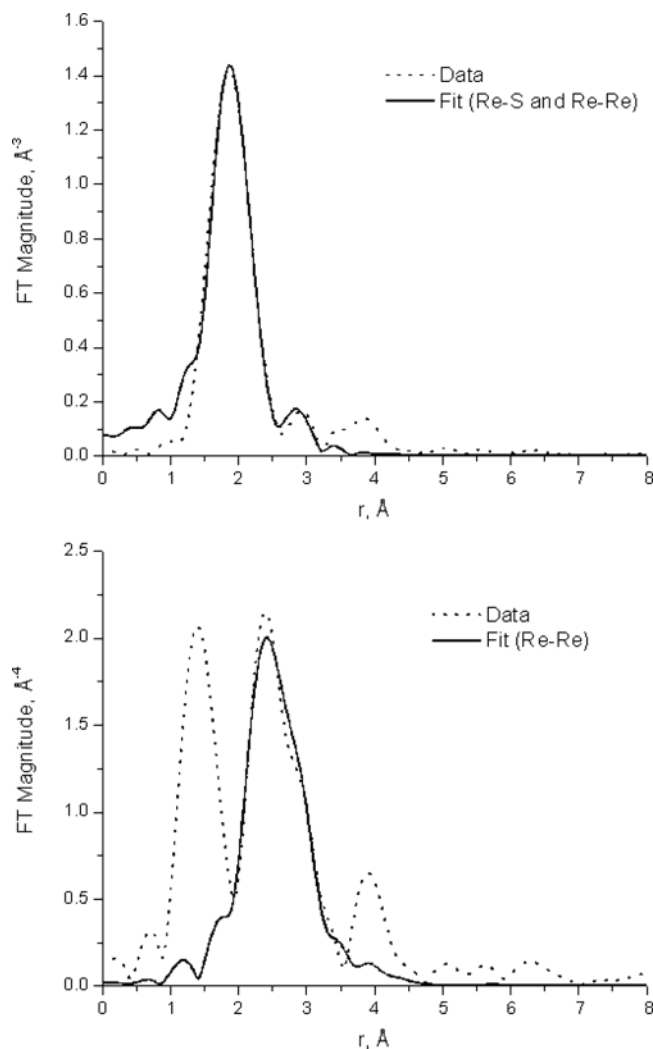

Figure 3. EXAFS fit for the Re−S and Re−Re shells (between 1.6 and 3.1 Å), using k^2-weighting and k-range from 2 to 10 Å^{-1} for both theory and the data for Re_2S_7 at 300 K (top), the subtraction of the best fit theory for the Re−S shell from the data (middle), and the fit to the remaining Re−Re shell (between 2 and 3.2 Å) using k^3-weightings and k-range from 2 to 9 Å^{-1} (bottom). The mismatch between the theory and the data below 1.6 Å in the top and bottom panes is off the fitting range and is an artifact of background removal.

Table 5. EXAFS Data for ReS_4 and Its Decomposition Products at 300, 373, 473, 543, 573, 673, and 723 K

	300 K	373 K	473 K	543 K	573 K	673 K	723 K
Re−S [Å]	2.34(2)	2.34(2)	2.366(7)	2.36(1)	2.35(1)	2.371(9)	2.379(7)
Re−Re [Å]	2.77(1)	2.75(1)	2.779(7)	2.77(1)	2.787(6)	NA^a	2.81(3)
CN Re−S	4.6(6)	4.6(7)	6.2(5)	6.8(1.2)	6.2(7)	5.3(8)	5.7(3)
CN Re−Re	2.8(5)	3.9(9)	2.3(3)	3.6(6)	2.6(3)	NA^a	1.7(1.5)
σ^2 (Re−S) [Å²]	0.006(2)	0.007(2)	0.008(1)	0.011(3)	0.009(2)	0.006(2)	0.0077(7)
σ^2 (Re−Re) [Å²]	0.006(1)	0.010(2)	0.006(2)	0.008(2)	0.009(1)	NA^a	0.010(4)

^{a} High noise level in some high-temperature data prevented analysis eV per unit increase in the oxidation of sulfur, i.e., ca.

Figure 4. EXAFS fits for the Re–S and Re–Re shells for ReS$_4$ at 300 K using k^2-weighting for the Re–S and Re–Re shells fitting between 1.6 and 3.1 Å and the k-range from 2 to 10 Å^{-1} (top), subtracting the best-fit theory of the Re–S shell from the data and then fitting the residual with Re–Re contribution only between 2 and 3.2 Å, using k^3-weighting and k-range from 3 to 10 Å^{-1} (bottom).

10 eV difference between sulfide (2471.3 eV for FeS) and sulfate (2483.1 eV for Na$_2$SO$_4$). In addition to ReS$_4$ and Re$_2$S$_7$, the standards FeS, FeS$_2$, and Na$_2$SO$_4$ were also analyzed.

Our results showed similar XANES spectra for ReS$_4$ and Re$_2$S$_7$, consistent with the presence of similar sulfur ligands in these materials. The main peak at 2472.7 eV is consistent with persulfide (S$^-$) sulfur. Furthermore, both spectra show a shoulder that becomes evident upon deconvolution (Figure 6).[45] This shoulder function was fit with peak at 2471.1 eV, which is in the range expected for S^{2-}. The relative intensities of the two peaks indicate the S$^-$/S^{2-} ratios of ca. 3.5:1.6 for Re$_2$S$_7$ and 3.5:1.8 for ReS$_4$. In addition to the main peaks, several other peak functions are required to fit the XANES spectra completely. These include an arctangent function representing electronic transition to the continuum and several nonspecific localized electronic transitions.[45] Elemental sulfur (S^0), which has a characteristic peak near 2473.1 eV, was not observed.

Variable Temperature Measurements. TGA measurements on ReS$_4$ revealed a major loss of weight at ~523 K followed by a more gradual loss up to 1073 K. The net weight loss corresponded to 26%. The weight loss calculated for the conversion of ReS$_4$ into ReS$_2$ is 20.4%. Our sample contained ~5% CHN; therefore, the total weight loss was anticipated to be 25.4%. The TGA for Re$_2$S$_7$ showed a weight loss of 22% over the range 385–535 K, corresponding to the conversion of Re$_2$S$_7$ to ReS$_2$.[46]

EXAFS measurements were conducted on a sample of Re$_2$S$_7$ as a function of temperature from 300 to 723 K (Table 4). Our EXAFS measurements indeed show the conversion of Re$_2$S$_7$ into a material with the bond lengths and coordination numbers similar to those found in ReS$_2$ (Tables 3 and 4).

EXAFS measurements were also made on a sample of ReS$_4$ and its decomposition products as a function of temperature from 300 to 723 K (Table 5).

The Re L$_{III}$ edge EXAFS for ReS$_4$ shows prominent features at ~2 and 3 Å due to the Re–S and Re–Re coordination shells, respectively. These data were analyzed at each temperature using protocols as were employed for Re$_2$S$_7$ data analysis. Both sets of data indicated that upon heating, both Re$_2$S$_7$ and ReS$_4$ material converted to ReS$_2$, consistent with the TGA data (Table 3).

We do not rule out the possibility that the Re–S coordination number is underestimated in ReS$_4$ and correspondingly its σ^2 is overestimated (Table 5), at the lower measurement temperatures since these quantities can be correlated in the fitting procedures. One reason to suspect an underestimation of the ReS CN is that the otherwise similar compound, Re$_2$S$_7$, has a Re–S coordination number larger and smaller σ^2 (Table 4) than those found in ReS$_4$ (Table 5).

Discussion

This report describes the characterization of one of two known rhenium sulfur phases, Re$_2$S$_7$, and the synthesis and structural characterization of the new phase ReS$_4$.

Synthesis. The electropolymerization of a binary metal sulfide is a reaction that is without precedence, although electrochemical methods have been employed with some success in the synthesis of other sulfur-rich TMS.[47] Perhaps most unusual is the noted facility of the reductive depolymerization of ReS$_4$; this behavior has not been observed previously for other metal sulfide phases. The large gap between the deposition and the re-reduction (stripping) potentials for ReS$_4$ suggests that the polymerization entails a substantial structural rearrangement, a finding that is in turn consistent with the XAS results. As has been discussed extensively

(41) Frenkel, A. I.; Wang, F. M.; Kelly, S.; Ingalls, R.; Haskel, D.; Stern, E. A.; Yacoby, Y. *Phys. Rev. B: Condens. Matter* **1997**, *56*, 10869–10877.

(42) Müller, A.; Krickemeyer, E.; Bögge, H. *Z. Anorg. Allg. Chem.* **1987**, *554*, 61–78.

(43) Pickering, I. J.; Prince, R. C.; Divers, T.; George, G. N. *FEBS Lett.* **1998**, *441*, 11–14.

(44) Vairavamurthy, A.; Manowitz, B.; Zhou, W.; Jeon, Y. *ACS Symp. Ser.* **1994**, *550*, 412–430.

(45) Vairavamurthy, A. *Spectrochim. Acta, Part A* **1998**, *54A*, 2009–2017.

(46) Nirsha, B. M.; Savel'eva, L. V.; Rekharskii, V. I. *Izv. Akad. Nauk SSSR, Neorg. Mater.* **1984**, *20*, 164–165.

(47) Bélanger, D.; Laperriere, G.; Marsan, B. *J. Electroanal. Chem.* **1993**, *347*, 165–183.

Electrosynthesis of ReS₄

Chem. Mater., Vol. 16, No. 1, 2004   **157**
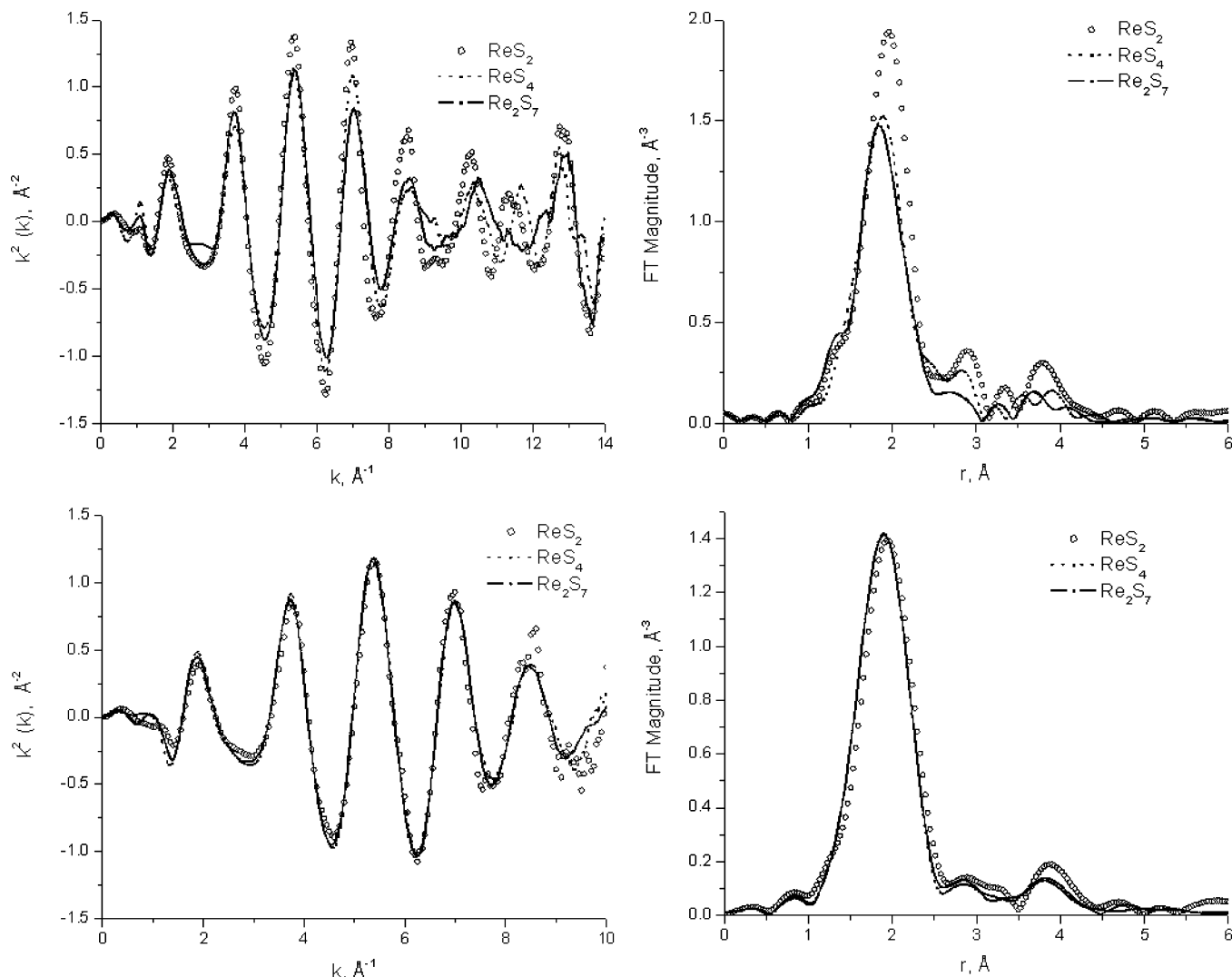
Figure 5. EXAFS data for the Re–S shell at 300 K for ReS₄, Re₂S₇, and ReS₂ (top row) and 700 K for ReS₂ and the decomposition products of ReS₄ and Re₂S₇ (bottom row). k^2-weightings and k-ranges between 2 and 12 Å^{-1} and between 2 and 9 Å^{-1} were used for the 300 K data and 723 K data, respectively, in Fourier transforms.

elsewhere, the oxidation of perthiometalates characteristically leads to reduction of the metal concomitant with coupling of the sulfido ligands. For example, the oxidation of MoS₄²⁻ gives [Mo₂(S₂)₆]²⁻ and [Mo₂S₄(S₂)₂]²⁻.[48]

Structural Proposals for Re₂S₇ and ReS₄. The fact that of our XAS analyses accurately reproduce the structural characteristics of the reference compounds ReS₂ and Et₄NReS₄ provided a critical test prior to the XAS analysis of the amorphous materials Re₂S₇ and ReS₄. The close similarity of Re₂S₇ and ReS₄ is strongly indicated by the XAS data, as well as their TGA behavior. Beyond these facts, the structural assignments for the local structures of the Re₂S₇ and ReS₄ phases were guided by the following considerations: (i) XAS data show the presence of both S²⁻ and S₂²⁻, with S²⁻ being less abundant than S₂²⁻. Sulfur is not present as S⁰ (see S₃²⁻ as found in (C₅Me₅)Re(S₃)Cl₂).[49] (ii) Rhenium sulfides of nuclearity >2 characteristically contain triply bridging μ₃-S.[18] (iii) Whereas EXAFS cannot distinguish μ₂-S vs μ₃-S, the absence of short Re–S contacts combined with the unimodal distribution

of Re–S bond lengths rules out terminal sulfides ($r_{Re=S}$ ∼ 2.14 Å). (iv) The Re oxidation state is expected to lie between 4⁺ (as in ReS₂) and 5⁺. The anion ReS₄⁻ is the unique example of a Re^VII sulfide, but it is stabilized by four terminal sulfido ligands, which are powerful π-donor ligands. At the other extreme, the octahedral Chevrel-like rhenium sulfide clusters exist in the 3⁺ oxidation state,[18] but this structure type is inconsistent with the EXAFS data.

The above considerations lead to two idealized compositions (based on integral Re oxidation states) for Re₂S₇: Re^IV(S)₀.₅(S₂)₁.₅ and Re^V(S)₁.₅(S₂)₁. Correspondingly, two idealized formulas are indicated for ReS₄, Re^V-(S)₁(S₂)₁.₅, and Re^VI(S)₂(S₂)₁. EXAFS measurements indicate that Re₂S₇ and ReS₄ may differ in the degree of Re–Re bonding (CN of ∼2 and ∼3, respectively), although it is difficult to rationalize more than two localized Re–Re bonds per d² metal center. The proposed structures are proposed to be members of a stoichiometric continuum Re^V(S)₁.₅₋₁(S₂)₁₋₁.₅ that differ in the S²⁻/S₂²⁻ ratio (Figure 7).

The structures proposed for Re₂S₇ and the new phase ReS₄ are interesting from a number of perspectives. Low-dimensional structures of this sort are consistent

(48) Stiefel, E. I. *Pure Appl. Chem.* **1998**, *70*, 889–896.

(49) Herberhold, M.; Jin, G. X.; Milius, W. *Z. Anorg. Allge. Chem.* **1994**, *620*, 299–303.
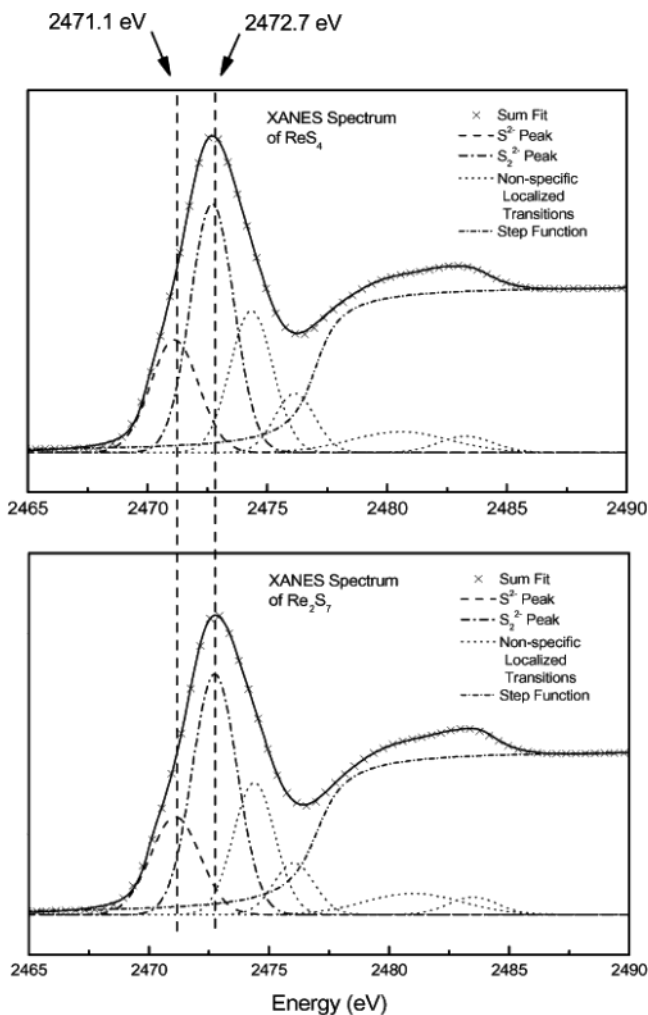
Figure 6. Fits for the S K-edge data showing the presence of sulfur as S^{2-} (2471.1 eV) and S^- in ReS$_4$ (2472.7 eV).

with the finding that ReS$_4$ can be reversibly reduced (albeit with significant overpotential) to ReS$_4^-$. A low-dimensional structure may also be relevant to the high catalytic activity of Re$_2$S$_7$, due to the intrinsically higher surface area. One attraction to such sulfur-rich phases
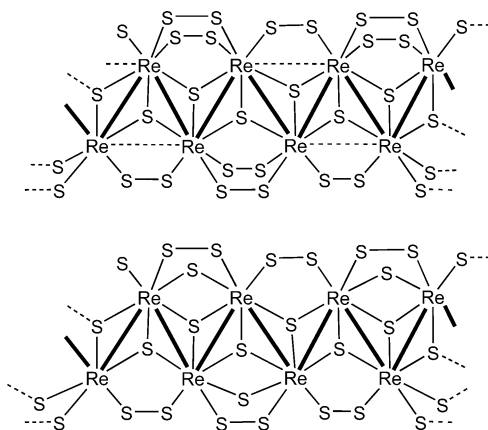
Figure 7. Structural proposal for Re$_2$S$_7$ (top) and ReS$_4$ (bottom), with the compositions Re^V(S)$_{1.5}$(S$_2$)$_1$ and Re^V(S)(S$_2$)$_{1.5}$, respectively.

is that they should be amenable to surface functionalization exploiting the reactivity inherent in the persulfido (S$_2^{2-}$) functionality.[50,51] These considerations encourage us to further explore electrochemical routes to other sulfided phases from other sulfur-rich monomers and their surface functionalization.

CM034467V

(50) Bolinger, C. M.; Weatherill, T. D.; Rauchfuss, T. B.; Rheingold, A. L.; Day, C. S.; Wilson, S. R. *Inorg. Chem.* **1986**, *25*, 634.
(51) Seyferth, D.; Henderson, R. S.; Song, L. C. *Organometallics* **1982**, *1*, 125−133.